

STRUCTURE AND MECHANICAL AND ELECTROCHEMICAL PROPERTIES OF ULTRAFINE-GRAINED Ti

Yu. R. Kolobov, O. A. Kashin, E. E. Sagymbaev, E. F. Dudarev, L. S. Bushnev,
G. P. Grabovetskaya, G. P. Pochivalova, N. V. Girsova, and V. V. Stolarov

UDC 539.43

A study is conducted into the microstructure and physico-mechanical properties of ultrafine-grained titanium produced by severe plastic deformation using the method of equichannel angular pressing. The effects of thermal and mechanical treatment on these characteristics are investigated. The possibility of forming mechanical properties in titanium that compare well with those of highly doped titanium alloys is shown.

INTRODUCTION

The unique mechanical and physico-chemical properties of ultrafine-grained materials are attracting an increasing amount of attention from researchers [1–8]. These properties are, above all, high-yield stress and strength accompanying satisfactory plasticity characteristics, the possibility of superplastic behavior at relatively low temperatures and strain rates, and considerably altered physical parameters.

Today, a number of processes are used to produce ultrafine-grained (UFG) metals and alloys. Among them, severe plastic deformation by equichannel angular pressing (ECAP) is believed to be the most promising method [3, 4].

Using a number of metals and alloys as an example, it has been shown that this technique for obtaining a UFG-structure can considerably enhance resistance to plastic deformation and wear developing under static and cyclic loading [2–4, 7–9]. The mechanisms underlying alteration of elastoplastic properties in the course of transformation of a polycrystalline structure into an ultrafine-grained one have not been identified yet.

The UFG-structures produced via the above method are characterized by high stored energy and non-equilibrium grain boundaries, which may lead to their structural transformations under certain temperature and loading conditions coupled with a redistribution of the dopants and interstitial impurities. This, in turn, brings about changes in the physical and elastoplastic properties. The data on the effects of thermal-mechanical treatment of UFG-materials on their structure and properties are available only for a few metals and alloys.

Taking the above features into consideration, we have carried out a series of investigations aimed at identifying the relationship between the microstructure of UFG titanium and its properties, i.e., strength and plasticity under static loading and fatigue strength and corrosion resistance, including those following thermal-mechanical treatment.

MATERIALS AND METHODS

The material investigated was commercial-grade titanium (initial titanium-IT) (composition in wt.% 0.12 O, 0.18 Fe, 0.07 C, 0.04 N, and 0.01 H) in untreated recrystallized (grain size $d = 10 \mu\text{m}$) and UFG states. The latter was achieved using severe plastic deformation (SPD) by ECAP [4] of the base recrystallized rods 20 mm in diameter followed by thermal-mechanical treatment. For different structural states, the yield strength $\sigma_{0.2}$, the tensile strength σ_t and the deformation to failure σ were determined at room temperature at a strain rate of 10^{-3} s^{-1} .

To measure microplastic deformation under quasistatic loading, use was made of the “loading-unloading” scheme for uniform bending of a flat specimen measuring $46 \times 6 \times (0.2-0.3) \text{ mm}$ in a preset radius mandrel [10]. Cyclic testing was carried out on the same machine under constant-sign loading from zero at a cycling frequency of 1.7 Hz while measuring the residual deformation to an accuracy of $5 \cdot 10^{-7}$.

The electrochemical properties of titanium were studied in a medium close in its composition to biological fluid (physiological solution at 37 °C) [11–13]. Under study was the behavior of the electrode potential and the change of the latter

Institute for Strength Physics and Materials Science; Siberian Physical-Technical Institute at Tomsk State University; Institute of Physics of Advanced Materials at UFA Aviation Technology University. Translated from *Izvestiya Vysshikh Uchebnykh Zavedenii, Fizika*, No. 2, pp. 77–85, January, 2000. Original article submitted August 26, 1999.

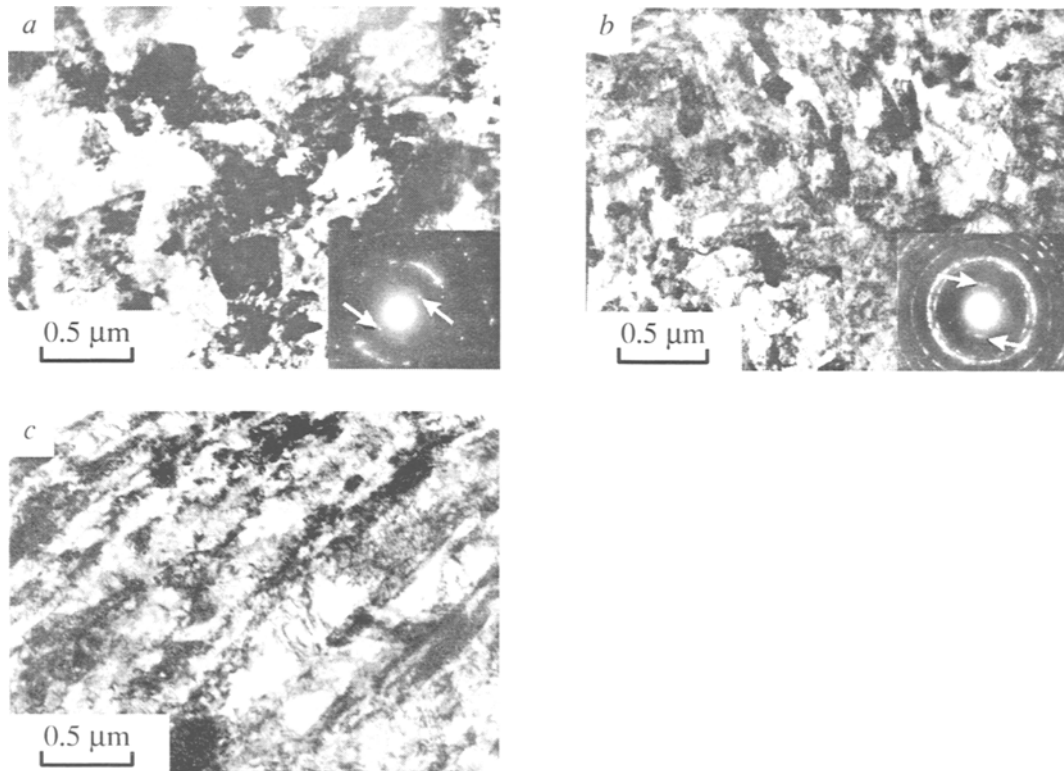


Fig. 1. Microstructure of titanium samples in the UFG-0 (*a*) and UFG-1 states in cross section (*b*) and longitudinal section (*c*). Arrows show superslattice reflections.

in polarization (passage of a current of certain density through the specimen), which is a characteristic of the kinetics of the electrode processes. The specimens used were plates measuring $50 \times 6 \times 0.5$ mm with a polished surface, the surface area of the submerged part being 200 mm^2 . For comparison, use was made of a reference chlorine-silver electrode and an auxiliary electrode made of commercially pure graphite. The current density used in polarization of the specimen was $50 \mu\text{A}/\text{mm}^2$.

The structure of titanium was investigated using an EM-126K transmission microscope at an accelerating voltage of 125 kV. The microstructure and mechanical and electrochemical properties of titanium were examined both in the untreated recrystallized state and following SPD through the ECAP method using different procedures. The ECAP modes were varied in order to achieve maximum values of the mechanical properties – strength, plasticity, and fatigue limit. To do so, further mechanical and heat treatment of varying modes followed the ECAP. For the sake of convenience, we use the following acronyms in this paper:

IT is the base recrystallized titanium with average grain size $d \approx 10 \mu\text{m}$;

UFG-0 is the titanium upon the ECAP;

UFG-1 is the titanium upon the ECAP followed by severe plastic deformation;

UFG-2 is the titanium upon the ECAP followed by severe plastic deformation and prior-to-recrystallization annealing.

EXPERIMENTAL RESULTS

The microstructure of polycrystalline titanium, used as a base material for the production of UFG-states, was typical of recrystallized metals with distinct grain boundaries.

The average grain size was $10 \mu\text{m}$ and the dislocation density was small, around 10^{12} m^{-2} . For UFG-0, the grain size decreases so much that it becomes difficult to define it from metallographic specimens. The average grain size was measured from the electron micrographs as the size of the regions exhibiting similar contrast (Fig. 1*a*). (It should be noted that the

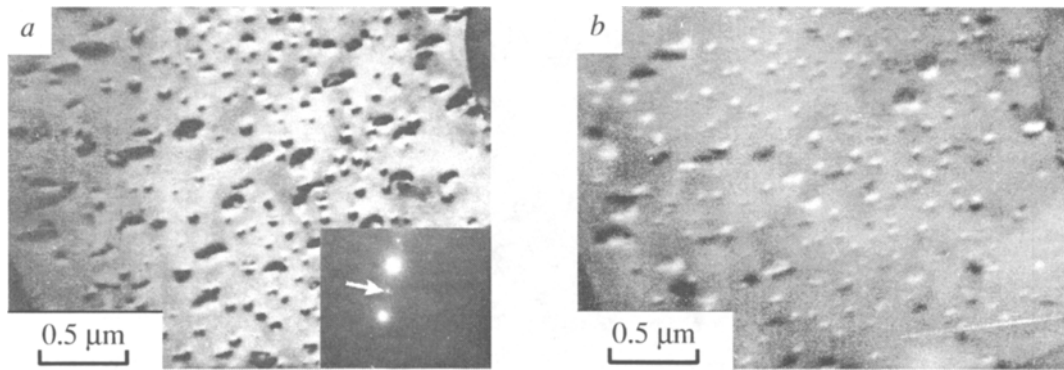


Fig. 2. Structure of UFG-titanium upon annealing at 500°C for 0.5 h: light-field micrograph, arrow shows the [0001] extra reflection (a), dark-field micrograph from the extra reflection marked (b).

TABLE 1. Mechanical Properties of Investigated Materials

Material	σ_t , MPa	$\sigma_{0.2}$, MPa	δ , %	H_m , MPa	σ'' , MPa
IT	464	360	24.8	1630	110
UFG-0	716	654	18.9	2300	210
UFG-1	1000	947	8.8	2780	140
UFG-2	960	860	10.6	2950	310

method used may underestimate the size because regions of similar contrast are likely to be surrounded by low-angle boundaries as well.) The measurements have shown a bimodal grain-size distribution in the material in question. The average size of fine grains was 0.3–0.35 μm . Coarse grains were up to 1 μm , with their volume fraction roughly estimated to be 40%. The dislocation density inside the coarse grains was the same as in the recrystallized state, which allows us to assume dynamic recrystallization to occur in the course of the ECAP treatment. In fine grains, the dislocation density was by far higher, up to $4 \cdot 10^{14} \text{ m}^{-2}$. The extinction contours evident in the micrographs testify to the presence of internal stresses.

The UFG-3 state is characterized by grains elongated in the direction of straining (Fig. 1, *b* and *c*). In the cross section, the grain shape was almost equiaxial and the average size was found to be $0.26 \pm 0.07 \mu\text{m}$. No coarse grains are seen. The longitudinal size of the grains was increased up to 0.6–1.5 μm . The dislocation density inside the grains has increased by about two orders of magnitude as compared to the starting coarse-grained titanium, with occasional grains exhibiting low dislocation density.

Annealing prior to recrystallization (UFG-2 state) has virtually no effect on the grain size versus the UFG-1 state, while the dislocation density slightly decreases and some of the grains become nearly free from dislocations. Recrystallization of the UFG-3 structure and grain growth up to 2–4 μm are observed upon isothermal annealing at 500°C.

The IT titanium specimens both in the starting and UFG-3 states exhibit a special feature, the frequent occurrence of extra reflections oriented as [0001], otherwise prohibited for titanium by the structural factor (Fig. 1 *a* and *b*). An analysis of these reflections has shown that they are matched by the mainstream reflections [0002], with the hexagonal α -titanium lattice parameter increased by 5–7%. Similar extra reflections are also found in the electron micrographs of recrystallized grains following annealing of the UFG specimens at 500°C for 0.5–1 h. These grains also display coherent disk-like precipitates producing the deformation contrast due to elastic distortions in the base-material lattice (Fig. 2 *a*). The dark-field micrographs confirm that the extra reflections [0001] result from the above precipitates (Fig. 2 *b*).

The mechanical characteristics of titanium in different states are listed in Table 1. It is evident from the table that as a result of transformation from the coarse to the UFG-0 state, $\sigma_{0.2}$ and σ_t increase by a factor of 1.5–2, while plasticity is somewhat decreased. The subsequent deformation (state UFG-1) tends to dramatically reduce the sample relative elongation to failure.

Annealing prior to recrystallization (state UFG-2) slightly decreases σ_t and $\sigma_{0.2}$ while causing an insignificant increase in δ . The considerable decrease in σ_t and $\sigma_{0.2}$ and the growth in δ are observed following the annealing of the UFG titanium at

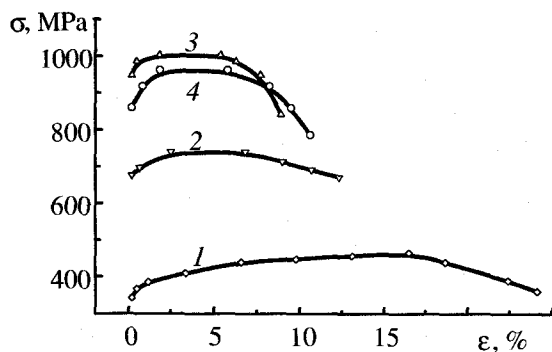


Fig. 3

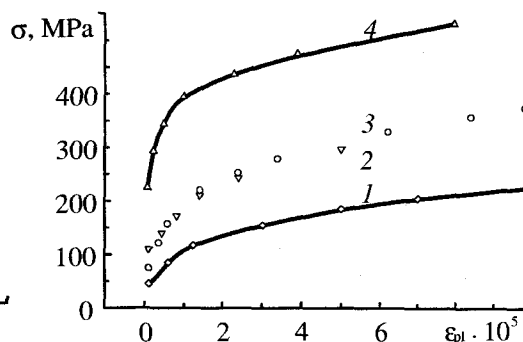


Fig. 4

Fig. 3. Tension curves for titanium in the IT (1), UFG-0 (2), UFG-1 (3), and UFG-2 (4) states.

Fig. 4. Curves for microplastic deformation buildup in titanium in the IT (1), UFG-0 (2), UFG-1 (3), and UFG-2 (4) states under quasistatic loading.

500°C. The microhardness of titanium in state UFG-0 is by a factor of 1.5 higher than that in the as-prepared recrystallized IT state. Continued thermal and mechanical treatment causes the microhardness to increase further.

Figure 3 shows the σ - ϵ tensile curves for the titanium samples tested in all states in question at room temperature. For the recrystallized IT titanium (curve 1), we observe a lengthy initial stage with a low work-hardening coefficient followed by the stage of decreasing stress. The initial section of the UFG-0 titanium of the σ - ϵ curve (curve 2) is characterized by a high work-hardening coefficient. The latter drops to zero already at $\epsilon = 2-6\%$, which is followed by the stage of decreasing flow stress σ seen in the σ - ϵ curve. The tensile curves for the UFG-1 and UFG-2 titanium (curves 3 and 4, respectively) behave similarly to those for the UFG-0 titanium.

The evolution of plastic deformation and fracture occurs differently for the samples of the coarse-grained and UFG titanium. Initially in the IT titanium sample subjected to deformation, a weakly pronounced neck is formed, which covers the entire working part of the sample. This is accompanied by the formation of a localized neck. In the tensile curve, the onset of the second neck scales with the decrease in the flow stress (at $\approx 17\%$). Failure occurs in the localized neck through fracturing along the plane normal to the axis of tension. In the UFG-0 titanium undergoing deformation, we also observe a neck being formed across the entire working part of the sample at the beginning, which is, however, followed by the formation and development of one and then another localized shear macroband. Their appearance is reflected in the σ - ϵ curve as the onset of the declining stress stage. The macrobands are located 90° to each other and 45° with respect to the axis of tension. The ultimate failure occurs through shearing along one of the localized shear macrobands. States UFG-1 and UFG-2 are characterized by the formation of localized plastic deformation macrobands already at low degrees of straining avoiding the preliminary necking, with all the deformation-to-failure being localized in a narrow band.

The character of the macroplastic deformation buildup in the as-prepared recrystallized IT titanium is shown in Fig. 4 (curve 1). Similar to other polycrystalline materials [14-16], macroplastic deformation builds up in two stages: in the first stage, the growth of deformation with stress follows a linear law, and in the second stage it becomes parabolic.

Irrespective of the method of manufacture and subsequent treatment techniques, the titanium samples in all UFG states under study in the microplastic deformation zone behave in a fashion similar to the starting recrystallized titanium: they exhibit a linear relationship between stress and deformation in the first stage and a parabolic one in the second (Fig. 4, curves 2-4). From Table 1 it is, however, evident that the macroplastic elastic limit σ'' of the UFG titanium is always higher than that of the coarse-grained one. The value of the excessive stress depends on the method of treatment. The macroscopic elastic limit in state UFG-0 increases nearly twice, while in state UFG-1 it decreases. In state UFG-2, σ'' is maximum, and it is three times that of the coarse-grained titanium. Under cyclic loading, the buildup of residual deformation is determined as the number of cycles is increased (Fig. 5). For all the states, it follows a logarithmic law, with a sharply enhanced intensity of the process prior to failure (Fig. 5, curves 4 and 6).

It is noteworthy that from the onset of the increase in the deformation buildup to ultimate failure, the material under study cannot endure more than $(1-3) \cdot 10^4$ cycles. As the maximum cyclic stress grows, both the absolute residual deformation and its buildup rate increase as well.

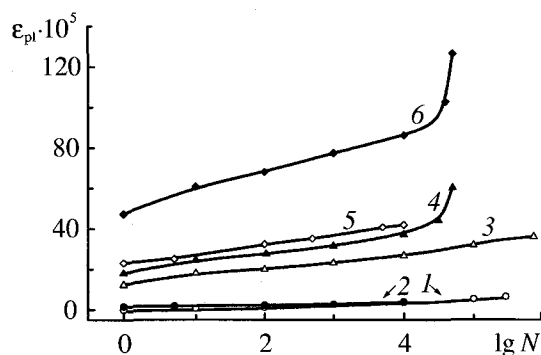


Fig. 5. Microplastic deformation buildup in different titanium samples under cyclic loading versus number of cycles (1, 5) – IT, (2) – UFG-0; (3, 6) – UFG-1, (4) – UFG-2. Maximum initial cycle stress: (1) – 122, (2) – 260; (3) – 417, (4) – 625, (5) – 288, and (6) – 625 MPa.

TABLE 2. Fatigue Properties of Investigated Materials

Material	σ_{max} , MPa	No.	σ_{max}/σ''	$\sigma_{max}/\sigma_{0.2}$
IT	122	$>10^6$	1.1	0.34
	351	$>10^6$	3.2	0.98
	351	$40 \cdot 10^4$	3.2	0.98
	362	$2 \cdot 10^4$	3.3	1.01
	375	$42 \cdot 10^4$	3.4	1.04
	430	$2 \cdot 10^4$	3.9	1.2
UFG-0	260	$>10^6$	1.2	0.4
	509	$>10^6$	2.4	0.78
	598	$2 \cdot 10^4$	2.8	0.91
UFG-1	417	$>10^6$	3	0.44
	520	$>10^6$	3.7	0.55
	534	$18.5 \cdot 10^4$	3.8	0.56
	552	$9 \cdot 10^4$	3.9	0.58
	562	$12 \cdot 10^4$	4	0.59
	573	$25 \cdot 10^4$	4.1	0.61
UFG-2	469	$>2.1 \cdot 10^6$	1.5	0.55
	520	$>10^6$	1.7	0.6
	625	$6 \cdot 10^4$	2	0.73

The value of the residual deformation after the same number of cycles and the same starting stress amplitudes will always be lower for the UFG titanium (Fig. 5, curve 1) than for the coarse-grained titanium (Fig. 5, curve 5). It is practically unaffected by severe plastic deformation (state UFG-1). Annealing prior to crystallization (state UFG-2) does, however, affect the residual deformation, and it decreases sharply (Fig. 5, curves 4 and 6). At the maximum cycle stress close to the macroscopic elastic limit, the residual deformation builds up very slowly, being as low as 10^{-4} after 10^5 cycles (Fig. 5, curves 1 and 2).

The results of fatigue loading of titanium in a variety of states and maximum cyclic stresses are listed in Table 2. It is clear from the table that the samples in all states in question and at maximum cyclic stresses m_{max} close to the macroscopic elastic limit σ'' do not fail even after 10^6 loading cycles. Note, however, that the fatigue limit based on 10^6 cycles is considerably higher (1.7–3.7 times) than σ'' for all samples studied. Comparing the maximum cyclic stress with the yield stress, we can see (Table 2) that the fatigue limit in the UFG titanium samples may be as high as $0.8 \sigma_{0.2}$, and for the coarse-

grained samples these values almost coincide. It might be well to point out that in all the UFG states, the fatigue limit in the samples subjected to 10^6 cycles did not exceed 500 MPa.

The study of the electrode potential of the IT and UFG titanium samples has shown that the time of their transformation into the passivated state is the same for all samples and equals 15–20 min. Within this time, the value of the potential changes by 100–120 mV and reaches 300 mV for the IT titanium and 270 mV for the UFG state. The ratio of potential variation to current density was 0.5 M Ω for the UFG state. The behavior of the potentiostatic curves of both samples is similar, which testifies to the formation on the UFG titanium surface of a passive oxide film similar to that on the surface of the as-prepared recrystallized IT titanium samples.

DISCUSSION OF RESULTS

The main distinguishing feature of UFG materials is the formation, during SPD treatment, of grains less than 1 μm in diameter surrounded by high-angle boundaries, which cannot be produced by conventional thermomechanical techniques. Unfortunately, our results do not yield an unambiguous answer to whether the zones of the same contrast in electron micrographs from the UFG titanium samples are the grains with high-angle boundaries. To prove this, special research is needed into the identification of misorientations in those regions. We may, nonetheless, ascertain that the ECAP method enables production in titanium of structural elements as small as 0.3–0.35 μm , which are reduced to a still finer size in the course of subsequent treatment. The resulting structure remains stable after short-term (0.5–1 h) annealing at temperatures up to 300°C.

A feature typical of the structure of the materials studied is the presence of superlattice reflections in the electron diffraction patterns from fine precipitates. It has been reported in the literature [17–20] that the presence of interstitial impurities (oxygen, nitrogen, or carbon) in titanium can significantly influence its mechanical performance. We are not aware of any investigations where this effect is attributed to the occurrence of precipitates. A likely explanation of the fact that these precipitates have been overlooked is that they seldom occur in coarse-grained titanium. The results of this work point to the presence of the said precipitates both in the starting and the UFG states. We can assume that the SPD treatment causes a redistribution of carbon in titanium because it is the least soluble impurity. If the carbon is distributed in a well-ordered fashion in a given microvolume of the material parallel to the base [0001] titanium planes with a single interplanar spacing, this will give rise to extra reflections of the [0001] type and an increase in the titanium lattice parameter. Provided this assumption is true, then, given the necessary thermodynamic conditions, the TiC phase will precipitate. At 500°C and lower, carbon is unlikely to form TiC, hence the metastable states described above. One may, therefore, expect that as a result of subsequent thermomechanical treatment of the UFG titanium, the latter will undergo carbon aging, which may dramatically modify the evolution of the dislocation structure in plastic deformation. The possibility of strain aging of commercially pure titanium has been reported elsewhere [17].

A distinguishing characteristic of the UFG titanium behavior is the formation of localized shear macrobands. These were also observed earlier during deformation of nanostructural [22] and UFG materials [23, 24]. However, there is no general agreement as to the causes of this localization of plastic deformation. To solve this issue, more data has to be collected and special experiments have to be staged.

Fatigue properties are decisive when choosing operating conditions for articles and parts working under cyclic loading. At the same time, the complete cycle of fatigue testing (construction of Wurler's curve) would require a great number of samples and a lot of time. For coarse-grained materials, it has been shown that it is possible to forecast the fatigue life of a material using the value of its macroscopic elastic limit in quasistatic testing [14–16]. These considerations have been detailed in [14, 25], where it was demonstrated that the macroscopic elastic limit and the fatigue life characterize the stress of plastic deformation transition from individual grains to a higher scale level – the cooperative plastic deformation of grain agglomerates. As follows from the experimental data obtained in the present work and in [25], the laws of microplastic deformation buildup in the UFG titanium under quasistatic and cyclic loading are the same as in the coarse-grained recrystallized IT titanium. The main point in the dependences obtained is considerable excess in the fatigue limit compared to the value of the macroscopic elastic limit. In the present work, σ'' has been defined as the stress at which one observes a deviation from the linear law of residual deformation buildup. This deviation can be related not only to the dislocation motion through grain boundaries but also to the presence of second-phase precipitates [26]. In addition, the occurrence in the material of different-type low- and high-angle boundaries should affect the mechanisms of residual deformation buildup. The measured σ'' values may not, therefore, be the true characteristics of the macroscopic elastic limit. One of our upcoming papers will concentrate on solving this issue.

CONCLUSIONS

The formation of an ultrafine-grained structure in commercially pure titanium by the ECAP method ensures its advanced mechanical properties. Further thermomechanical treatment of UFG titanium substantially changes its structural-phase state due to alterations in the dislocation structure, grain-boundary state, and aging effects. This leads to a change in its mechanical characteristics. Under moderate conditions of thermomechanical treatment, the strength properties of UFG titanium attain values typical of highly doped titanium alloys. The UFG structure controls the character of the evolution of plastic deformation and failure: in UFG titanium, we observe deformation localization at the macrolevel.

The corrosion behavior of UFG titanium in a physiological solution hardly differs from that of coarse-grained titanium. The formation of a passive oxide film on its surface similar to that on IT alloys provides high corrosion resistance in this medium.

The character of the microplastic deformation buildup in the UFG titanium under static and cyclic loading approaches that in the coarse-grained recrystallized IT titanium. The fatigue limit of the UFG titanium in different states based on 10^6 cycles is no less than the macroscopic elastic limit σ'' . This permits us, using the static testing results, to predict the lower bound of the UFG titanium fatigue limit. By means of thermomechanical treatment we can obtain the value of the fatigue limit of the UFG titanium based on 10^6 cycles to be over 520 MPa.

The strength characteristics of UFG-1 and UFG-2 titanium are in excess of those of a medical alloy of the American standard, Ti-6Al-4VELI, whose yield strength is 800 MPa and whose tensile strength is 860 MPa [21].

The results obtained allow us to recommend undoped commercial grade UFG-titanium to be used in orthopaedics and traumatology as an implant and prosthesis material.

This work was supported by the Russian Fund for Basic Research (grant No. 98-02-16517) and by Los Alamos National Laboratories.

REFERENCES

1. H. Gleiter, *Progr. Mater. Sci.*, No. 33, 223–315 (1989).
2. J. R. Weertman, *Mater. Sci. Eng.*, **A116**, No. 1997, 16–26 (1993).
3. R. Z. Valiev, N. A. Krasilnikov, and N. K. Tsenev, *Mater. Sci. Eng.*, **137**, 35 (1991).
4. Yu. R. Kolobov, G. P. Grabovetskaya, I. V. Ratochka, *et al.*, *Nanostructured Mater.*, **12**, 1127–1130 (1999).
5. Yu. R. Kolobov, G. P. Grabovetskaya, I. V. Ratochka, *et al.*, *Ann. Chim. Sci. Mater.*, No. 21, 483–491 (1996).
6. R. Z. Valiev, D. A. Salimonenko, N. K. Tsenev, *et al.*, *Scripta Materialia*, **37**, No. 12, 1945–1950 (1997).
7. K. V. Ivanov, I. V. Ratochka, and Yu. R. Kolobov, *Nanostructured Materials*, **37**, No. 12, 947–950 (1999).
8. R. Z. Valiev, *Mater. Sci. Eng.*, **A234–236**, 59–66 (1997).
9. A. Vinogradov, Y. Kaneko, K. Kitagawa, *et al.*, *Scripta Materialia*, **36**, No. 11, 1945–1950 (1997).
10. S. O. Tsobkallo and Yu. F. Balandin, *Measuring Devices*, No. 2, 26–31 (1959).
11. A. V. Karlov, Yu. R. Kolobov, L. S. Bushnev, *et al.*, *Topical Issues of Orthopaedics and Traumatology* [in Russian], Ufa (1997).
12. A. V. Karlov, Yu. R. Kolobov, L. S. Bushnev, and E. E. Sagymbaev, *Biomedizinische Technik*, **B42**, No. 2, 504–507 (1997).
13. R. Thull, *Naturwissenschaften*, No. 81, 481–488 (1994).
14. E. F. Dudarev, *Microplastic Deformation and Yield Points in Polycrystals* [in Russian], State University, Tomsk (1988).
15. N. N. Nikitina, G. P. Pochivalova, and O. B. Perevalova, *Probl. Prochn.*, No. 8, 40–44 (1979).
16. E. F. Dudarev, G. P. Pochivalova, and N. V. Nikitin, *Izv. Vyssh. Uchebn. Zaved., Fiz.*, No. 3, 29–34 (1990).
17. U. Zwicker, *Titanium and Its Alloys* [Russian translation], *Metallurgiya*, Moscow (1983).
18. B. N. Arzamasov (ed.), *Structural Materials Handbook*, [in Russian], *Mashinostroyeniye*, Moscow (1990).
19. V. A. Kolachev, *Physical Metallography of Titanium* [in Russian], *Metallurgizdat*, Moscow (1976).
20. V. A. Kolachev and A. V. Mal'kov, *Physical Principles of Fracture of Titanium* [in Russian], *Metallurgiya*, Moscow (1983).
21. *Standard Specifications for Wrought Titanium 6Al-4VELI Alloy for Surgical Implant Application* ASTM Designation: F136–92.
22. P. G. Sanders, G. J. Yongdall, and J. R. Weertman, *Mat. Sci. Eng.*, **A234–236**, 77–82 (1997).

23. V.E. Panin, L. S. Derevyagina, and R. Z. Valiev, *Fiz. Met. Metalloved*, **2**, Nos. 1–2, 89–95 (1999).
24. R. Sh. Musalimov and R. Z. Valiev, *Physical Mesomechanics*, No. 2, 98–100 (1992).
25. E. F. Dudarev, O. A. Kashin, Yu. R. Kolobov, *et al.*, *Izv. Vyssh. Uchebn. Zaved., Fiz.*, No. 12, 20–25 (1998).
26. E. F. Dudarev, *Plastic Deformation of Alloys* [in Russian], State University, Tomsk (1987).